# Free-Standing Lead Zirconate Titanate Nanoparticles: Low-Temperature Synthesis and Densification

Ashis Banerjee and Susmita Bose*

*School of Mechanical and Materials Engineering, Washington State University, Pullman, Washington 99164-2920*

*Received June 15, 2004. Revised Manuscript Received September 9, 2004*

Nanocrystalline lead zirconate titanate (PZT) powder with an average particle size between 70 and 110 nm was synthesized using the citrate nitrate (C/N) autocombustion method. Phase-pure perovskite PZT nanoparticles were characterized by XRD, BET surface area, DSC/TGA, and TEM analysis. The crystallite size of the PZT nanoparticles was found to be between 10 and 15 nm. The BET specific surface area increased with increasing C/N ratio during synthesis due to porous structure formation, as the free-standing nanoparticles started to agglomerate. Sintering studies of the pressed pellets made by pure PZT showed >97% theoretical density at 1200 °C for 20 min, whereas the same with 2 wt % ZnO-doped PZT nanoparticles showed 93% theoretical density at as low as 900 °C. Piezoelectric properties were measured using uniaxially pressed compacts at room temperature of these nanoparticles. The room temperature dielectric constant was 550, the piezoelectric constant ($d_{33}$) was 160 pC/N, and the coupling coefficient ($k_t$) was 0.35 for pure PZT nanoparticles. ZnO-doped PZT nanopowder showed a dielectric constant in the range of 1200−1250, and $d_{33}$ in the range of 155−170 pC/N and $k_t$ in the range of 0.32−0.34. Nanocrystalline PZT powder can be useful for low-temperature sintering.

## Introduction

Lead zirconate titanate (PZT) is one of the most widely used piezoelectric inorganic materials due to its excellent properties. PZT-based ceramic materials can be found in different important applications such as ultrasonic transducers for medical imaging, underwater communications, hydrophones, speakers, fish finders, sensors, actuators, electrical resonators, and wave filters. PZT is a solid solution of ferroelectric $PbTiO_3$ ($T_c$ = 490 °C) and antiferroelectric $PbZrO_3$ ($T_c$ = 230 °C). PZT has perovskite structure, and below its Curie temperature ($T_c$ = 350 °C) it is noncentrosymmetric. The best piezoelectric properties can be obtained near the morphotropic phase boundary, where the Zr:Ti ratio is 52:48 at room temperature.[1,2] The final sintered density, microstructure, doping, and composition can influence the properties of the PZT-based ceramics. The sintered density and microstructure are very much dependent on the synthesis process and the starting materials.[3−5] Several methods have been reported to make PZT-based materials. In case of solid-state methods,[6−8] the starting materials are oxides, carbonates, or hydroxides of Pb, Zr, and Ti. The particle size of these starting materials is in the micrometer or submicrometer range. The perovskite phase forming temperature of PZT is high (700−800 °C) compared to that of other processes, and also the particle size of the final PZT powder is in the range of micrometers or submicrometers. In this method stoichiometric nonhomogeneity may arise, which can affect the electrical and mechanical properties of the final sintered products. In the case of the sol−gel method,[9−11] the sol of $Pb^{2+}$, $Zr^{4+}$, and $Ti^{4+}$ is made by using the metal alkoxide of the respective elements in organic solvent. The sol is converted to a viscous gel by controlled hydrolysis. Drying of the gel followed by calcination gives the phase-pure PZT powder. The sol−gel method is widely used for PZT thin film preparation. In the hydrothermal method[12−15] PZT powder is synthesized in the particle size range of nanometers to micrometers. The advantages of this method are (1) no calcination steps, (2) a low-temperature process, and (3)

* To whom correspondence should be addressed. E-mail: sbose@wsu.edu.

(1) Jaffe, B.; Roth, R. S.; Marzullo, S. *J. Appl. Phys*. **1954**, *25*, 809−810.
(2) Kakegawa, K.; Mohri, J.; Shirasaki, S.; Takahasi, K. *J. Am. Ceram. Soc*. **1982**, *65*, 515−519.
(3) Chinang, S. S.; Nishioka, M.; Fulrath, R. M.; Pask, J. A. *Am. Ceram. Soc. Bull*. **1981**, *60* (4), 484−489.
(4) Zhang, Z.; Raj, R. *J. Am. Ceram. Soc*. **1995**, *78* (12), 3363−3368.
(5) Randall, C. A.; Kim, N.; Kucera, J. P.; Cao, W.; Shrout, T. R. *J. Am. Ceram. Soc*. **1998**, *81* (3), 677−688.
(6) Matsuo, Y.; Sasaki, H. *J. Am. Ceram. Soc*. **1965**, *48* (6), 289−291.
(7) Chandatreya, S. S.; Fulrath, R. M.; Pask, J. A. *J. Am. Ceram. Soc*. **1981**, *64* (7), 422−425.
(8) Shrout, T. R.; Papet, P.; Kim, S.; Lee, G. S. *J. Am. Ceram. Soc*. **1990**, *73* (7),1862−1867.
(9) Hirashima, H.; Onishi, E.; Nagakowa, M. *J. Noncryst. Solids* **1990**, *121*, 404−406.
(10) Zhou, Q. F.; Chan, H. L. W.; Choy, C. L. *J. Mater. Process. Technol.* **1997**, *63*, 281−285.
(11) Palkar, V. R.; Multani, M. S. *Mater. Res. Bull*. **1979**, *14*, 1353−1356.
(12) Cheng, H. M.; Ma, J. M.; Zhu, B.; Cui, Y. H. *J. Am. Ceram. Soc*. **1993**, *76* (3), 625−629.
(13) William, J. D. *Ceram. Bull.* **1988**, *67* (10), 1673−1678.
(14) Kutty, T. R. N.; Balachandan, R. *Mater. Res. Bull*. **1984**, *19* (11), 1479−1488.
(15) Lencka, M. M.; Anderko, A.; Riman, R. E. *J. Am. Ceram. Soc*. **1995**, *78* (10), 2609−2618.

10.1021/cm0490423 CCC: $27.50 
Published on Web 11/24/2004

excellent compositional control. Eiras et al.[16] and Komarneni et al.[17] have reported the synthesis of PZT powder by the coprecipitation method. This method is based on the precipitation of the constitutive element at a particular pH followed by calcination. Particle sizes of the PZT powders, prepared by the above-mentioned methods, are generally in the micrometer to submicrometer range. In recent years, researchers have focused on the synthesis of nanosized PZT powder particles to improve the final properties primarily due to better sintering at lower temperature and reduction of lead loss by reducing the sintering temperature. Lead volatilization at high temperature hinders the densification process and also makes it difficult to control the composition in the final body and reproducibility of the product with good piezoelectric properties. Excess lead affects the densification process and properties in the final product.[18−21] Clark et al.[19] reported that the presence of excess PbO enhanced the densification rate by forming a liquid phase in the initial and intermediate stage of sintering. But it lowers the densification rate in the final stage of densification. Sasaki et al.[20] reported that the compositional changes take place during sintering of PZT when excess PbO is used. PbO helps in liquid-phase sintering. But the solubility of the $TiO_2$ component in liquid PbO in PZT is higher than that of $ZrO_2$. Therefore, the composition of the PZT phase shifts toward the Ti-rich side when excess PbO is used. This also affects the properties of PZT.

The sol−gel method has been widely used to prepare nanoparticles, films, and bulk forms.[22,23] In our laboratory we have shown the feasibility of making nanoparticles using different template materials, with controlled morphologies and improved properties.[24−26] Of major concern in nanoparticle synthesis, especially for inorganic ceramics, is agglomeration of nanoparticles. Surfactant template systems, particularly reverse micelle systems, are reported to act as efficient nanoreactors for synthesis of inorganic nanoparticles.[27,28] Liu et al. have recently reported the synthesis of free-standing PZT particles of 10−30 nm size using an organic solution of metalloorganic precursors of metal ions via a modified sol−gel method.[29] However, all these wet chemical methods produce powder particles which need a high calcination temperature or a longer calcination time, which promote agglomeration. The synthesis of inorganic powder using the citrate nitrate autocombustion method can address some of these concerns. In this method, metal ions in aqueous medium form a chelated complex with citric acid in the presence of nitric acid. Partial evaporation of water during the heat treatment forms a gel, and further heating of this gel at higher temperature gives exothermic reaction between the metal ion-chelated citrate complex and nitrate, which helps to synthesize phase-pure crystalline powder. Qi et al. reported the synthesis of nanocrystalline $LaFeO_3$ with a particle size of about 30 nm using the sol−gel autocombustion method.[30] Marinsek and co-workers have used this method to form a Ni−YSZ cermet anode.[31] The synthesis of barium zirconate titanate powder with a particle size of about 1.36 $\mu$m was reported by Maiti et al., which involved autocombustion of a citrate nitrate gel route.[32] The typical surface area of these particles was 9.0 $m^2/g$, and they were sintered up to 92−93% density at 1300 °C.

The densification kinetics of PZT-based systems has been studied by several researchers by using dopants to reduce the densification temperature and time. Additives can enhance densification by the formation of a low-melting-point glassy phase, but often they may reduce other properties. Duran et al.[33] have reported the microstructure and electrical properties of ZnO-doped $BaTiO_3$, and Yoon et al.[34] reported densification behavior of ZnO-doped $BaTiO_3$. Dopant distribution as well as the nature of the dopant precursor played a key role in the microstructural development to achieve a homogeneous fine-grained microstructure.

In the present paper we report the synthesis method of PZT (52/48) nanoparticles by citrate nitrate autocombustion with controlled morphology at a temperature below 500 °C, which is comparatively lower than that of the other conventional PZT powder synthesis methods, which is usually above 700 °C. The advantage of this process is that it is not an expensive process and it does not need any special reaction environment or equipment. Moreover, morphology of nanoparticles can be controlled by changing the synthesis parameters. Effect of the citrate-to-nitrate ratio (C/N) and zinc oxide (ZnO) dopant on the final powder morphology and properties were also studied. The size of these nanoparticles primarily varied between 70 and 110 nm with a crystallite size of 10−15 nm. The powders were characterized by X-ray diffraction (XRD) analysis, thermal analysis (DSC and TGA), specific average surface area analysis using the BET method, and transmission electron microscopy (TEM). Keeping in mind that the addition of ZnO in the untrafine PZT nanoparticle system can potentially improve the densification properties as well as the electromechanical properties of PZT-based systems, sintering studies were conducted

(16) Bruno, A. M.; Eiras, J. A. *J. Am. Ceram. Soc*. **1993**, *76* (*11*), 2734−2736.
(17) Rama Mohana Rao, K.; Prasad Rao, A. V.; Komarneni, S. *Mater. Lett*. **1996**, *28*, 463−467.
(18) Guha, J. P.; Hong, D. J.; Anderson, H. U. *J. Am. Ceram. Soc*. **1988**, *71* (3), C-152−C-154.
(19) Kingon, A. I.; Clark, J. B. *J. Am. Ceram. Soc*. **1983**, *66* (4), 256−260.
(20) Kakegawa, K.; Matsunaga, O.; Kato, T.; Sasaki, Y. *J. Am. Ceram. Soc*. **1995**, *78* (4), 1071−1075.
(21) Song, B. M.; Kim, D. Y.; Shirasaki, S. I.; Yamamura, H. *J. Am. Ceram. Soc*. **1989**, *72* (5), 833−836.
(22) Livage, J.; Sanchez, C.; Babonneau, F. In *Chemistry of Advanced Materials*; Interrante, L. V., Hampden-Smith, M. J., Eds.; Wiley-VCH: New York, 1998; Chapter 9.
(23) Klabunde, K. J.; Mohs, C. In *Chemistry of Advanced Materials*; Interrante, L. V., Hampden-Smith, M. J., Eds.; Wiley-VCH: New York, 1998; Chapter 7.
(24) Bose, S.; Saha, S. K. *Chem. Mater*. **2003**, *15* (23), 4464−4469.
(25) Bose, S.; Saha, S. K. *J. Am. Ceram. Soc*. **2003**, *86* (6) 1055−57.
(26) Das, R. N.; Bandyopadhyay, A.; Bose, S. *J. Am. Ceram. Soc*. **2001**, *84* (10), 2421−23.
(27) Pileni, M. P. *Nat. Mater*. **2003**, *2*, 145.
(28) Pileni, M. P. *Langmuir* **1997**, *13*, 3266.
(29) Liu, C.; Zou, B.; Rondinone, A. J.; Zhang, Z. J. *J. Am. Chem. Soc*. **2001**, *123*, 4344−4345.
(30) Qi, X.; Zhou, J.; Yue, Z.; Gui, Z; Li, L. *Mater. Chem. Phys*. **2002**, *78*, 25−29.
(31) Marinsek, M.; Zupan, K.; Maeek, J. *J. Power Sources* **2002**, *106*, 178−188.
(32) Chakrabarti, N.; Maiti, H. S. *J. Mater. Chem*. **1996**, *6* (7), 1169−1173.
(33) Caballero, A. C.; Fernandez, J. F.; Moure; Duran, P. *J. Eur. Ceram. Soc*. **1997**, *17*, 513−523.
(34) Yoon, K. H.; Kim, J. W.; Jo. K. H. *J. Mater. Sci. Lett*. **1989**, *8*, 153−156.

at different temperatures by measuring the densities of the sintered compacts. Dielectric constants, piezoelectric constants ($d_{33}$), and coupling coefficients ($k_t$) were measured at room temperature. To the best of our knowledge this is the first time the synthesis of PZT nanoparticles with controlled morphology, from free-standing to agglomerated, has been reported using the citrate nitrate autocombustion method. This method may be useful to produce free-standing nanoparticles of PZT on a larger scale, and these PZT nanoparticles can be used for low-temperature sintering, which makes them useful for application on a wide range of substrates.

## Experimental Section

Lead nitrate (99.999%, Sigma, Missouri), zirconyl nitrate hydrate (99.99%, Aldrich, Wisconsin), and titania (Rutile 94%, Dupont, Delaware) powders were used as starting materials to make PZT ($Pb(Zr_{0.52}Ti_{0.48})O_3$). All chemicals were used without any further purification. Aqueous solutions of $Pb^{2+}$, $Zr^{4+}$, and $Ti^{4+}$ ions were first mixed in the required proportions. To make a 0.5 M lead nitrate ($Pb(NO_3)_2$) solution with 5% excess $Pb^{2+}$, to compensate for the Pb loss, 43.47 g of $Pb(NO_3)_2$ was dissolved in 250 mL of distilled water. To standardize the $Zr^{4+}$ amount in zirconyl nitrate hydrate ($ZrO(NO_3)_2{\cdot}xH_2O$), 1 g of zirconyl nitrate starting salt was dissolved in 10 mL of water. A clear and homogeneous solution was achieved by adding 10 mL of concentrated (15.8 N) nitric acid ($HNO_3$; Fisher Scientific, New Jersey) to this solution followed by heating at 80−100 °C with continuous stirring on a magnetic stirrer. After complete dissolution, the resulting solution was cooled to room temperature, and ammonium hydroxide ($NH_4OH$; J. T. Baker, New Jersey) was added to adjust the pH between 10 and 11 for complete precipitation. Precipitate was filtered out and calcined at 900 °C for 2 h. The amount of $Zr^{4+}$ present in the calcined product ($ZrO_2$) was calculated by weighing the sample, which gave the amount of $Zr^{4+}$ ion present in the zirconyl nitrate hydrate. Then 0.25 M $Zr^{4+}$ ion solution was prepared by dissolving 21 g of zirconyl nitrate hydrate in 25 mL of distilled water with the addition of 225 mL of concentrated (15.8 N) nitric acid ($HNO_3$). The solution became clear and homogeneous when heated at 80−100 °C with continuous stirring. To prepare a $Ti^{4+}$ solution, first titania ($TiO_2$) powder was kept for 4 days in hydrofluoric acid (HF; J. T. Baker, New Jersey). The liquid part was taken out by filtering the mixture. Excess ammonium hydroxide was added to the filtered liquid for complete precipitation. The precipitate was washed with distilled water and then dissolved in concentrated (15.8 N) nitric acid to form a clear solution of $Ti^{4+}$ ion. To standardize the solution, 10 mL of this solution was taken in a beaker, and ammonium hydroxide was added to the solution until complete precipitation. The precipitate was filtered and fired in an alumina crucible at 800 °C for 2 h. From the calcined product ($TiO_2$), the amount of $Ti^{4+}$ ion was calculated. Then by adding distilled water, a 0.5 M $Ti^{4+}$ ion standard stock solution was prepared. A PZT precursor solution ($Pb(Zr_{0.52}Ti_{0.48})O_3$) was prepared by mixing 40 mL of $Pb^{2+}$ solution, 41.6 mL of $Zr^{4+}$ solution, and 19.2 mL of $Ti^{4+}$ solution. The total amount of nitrate present in the precursor mixture was calculated from the amount of nitric acid present in the mixture and the amount of nitrate coming into the solution from the salts. Then citric acid ($C_6H_8O_7{\cdot}H_2O$, 99.9%, J. T. Baker, New Jersey) solution was added to this precursor mixture with citrate-to-nitrate ratios (C/N) of 0.5, 1, and 1.5. The resulting solution was kept on a hot plate between 80 and 100 °C with continuous stirring. When the gelation started, the hot plate temperature was increased to 450 °C. After complete drying the gelatinous mass started to burn, and after completeburning PZT powder was formed. To make the PZT nano-
powder carbon-free, it was calcined at 500 °C for 15 min. For ZnO-doped nanopowders, the required amount of zinc nitrate ($Zn(NO_3)_2{\cdot}6H_2O$, 99.2%, J. T. Baker, New Jersey) was added to the PZT precursor mixture, and then powder was synthesized using the same citrate nitrate method. The C/N ratio was kept at 0.5.

The powder was characterized for its phase purity at room temperature by XRD analysis using a Philips PW 3040/00 X'pert MPD system with Co Kα radiation and a Ni filter over the $2\theta$ range of 20−70° at a step size of 0.02° ($2\theta$) and a count time of 0.5 s per step. Thermal analysis was done using an STA 409 PC (Netzsch, Germany) system to study the different reaction steps and temperature of the PZT gel. This was done from room temperature up to 900 °C in the compressed air environment with a heating rate of 5 °C/min. The powder surface area was measured using a five-point BET surface area analyzer (Tristar 3000, Micromeritics, Georgia). Before the surface area was measured, all the samples were dried in the sample holder at 200 °C for 2 h, in the presence of flowing $N_2$. The powder morphology and particle size were evaluated using a transmission electron microscope (JEOL, JEM 120). The particle size distribution was measured using a particle size analyzer (NICOMP 380). The sintering was carried out in two stages. The samples were first presintered at 950 °C with a heating rate of 5 °C/min and a hold time of 30 min. Then they were heated to the final sintering temperature with a heating rate of 10 °C/min and sintered for 20 min. The final sintering temperatures were varied between 1100 and 1200 °C. After cooling, the densities of the samples were measured. For ZnO-doped PZT nanopowders, 0.1, 0.5, 1.0, 1.5, 2.0, and 5 wt % ZnO in PZT were studied. The electrical characterization of the highest density sample was done after poling at 100 °C with an applied voltage of 50 kV/cm. The dielectric constant was determined by measuring the capacitance by using an LCZ meter (KEITHLEY 3321) and from the sample dimension. $d_{33}$ was measured using a $d_{33}$ meter (SENSOR 0643 Piezo-d-meter), and $k_t$ was measured by using an impedance analyzer (Agilent 4294A, Precision impedance analyzer).

## Results and Discussion

The citrate nitrate autocombustion synthesis is a low-temperature synthesis process. This autocombustion process is an oxidation−reduction-type exothermic reaction, in which nitrate ions act as an oxidant and carboxyl groups of citric acid act as a reducing agent. The citric acid plays two different roles in this reaction; one is as a chelating agent, and the other is to provide the fuel for the autocombustion synthesis. The mixture contains a large amount of nitrate groups. When nitrate starts to decompose, it liberates oxygen gas. This oxygen acts as an in situ oxidizing agent and helps the carbon which is present in the citric acid to burn. Once carbon starts burning, it produces $CO_2$ gas. This reaction is exothermic, which is responsible for the increase in the temperature of the mixture at the micro level. The increase in temperature helps to burn more carbon in the mixture within a short period of time. Therefore, once the reaction starts, it does not need any further heating from the outside. The overall oxide-based reactions are[31]

$$9Pb^{2+} + 18NO_3^- + C_6H_8O_7 \rightarrow 9PbO + 18NO_2 + 6CO_2 + 4H_2O$$

$$9Zr^{4+} + 36NO_3^- + 2C_6H_8O_7 \rightarrow 9ZrO_2 + 36NO_2 + 12CO_2 + 8H_2O$$

$$9Ti^{4+} + 36NO_3^- + 2C_6H_8O_7 \rightarrow 9TiO_2 + 36NO_2 + 12CO_2 + 8H_2O$$

However, the chemical reaction of PZT formation is more complicated. Probably, first it forms $PbTiO_3$ and

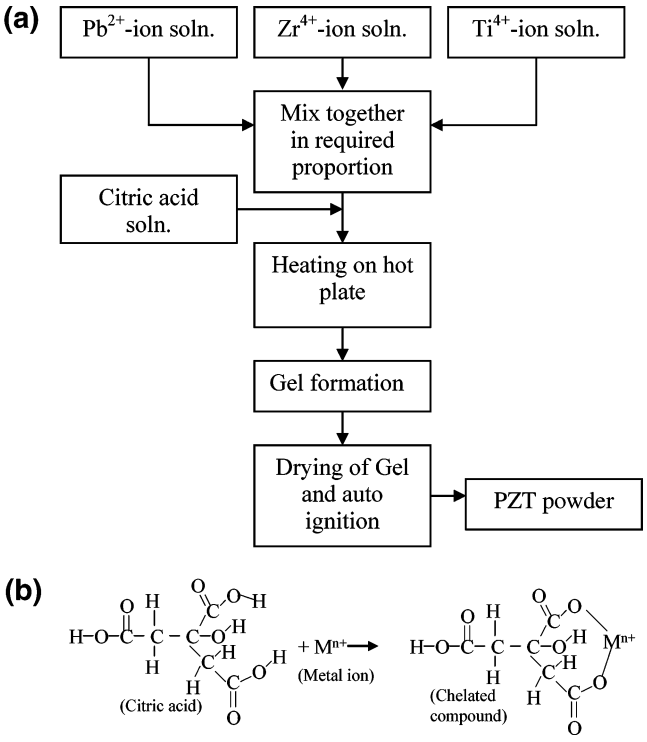


**Figure 1.** Synthesis of PZT nanoparticles by the citrate nitrate autocombustion method (a). Chelation mechanism of citric acid with metal ion (b).

$PbZrO_3$, and then PZT, from the solid solution of $PbTiO_3$ and $PbZrO_3$.[6,35] In the present system, phase-pure perovskite PZT forms without any further calcination. The hot plate temperature was kept at 450 °C to speed up the reaction and remove the maximum amount of carbon at the same time during the synthesis. To achieve carbon-free PZT nanoparticles, calcination was done at 500 °C for 15 min in a muffle furnace in an air environment. This calcination was carried out to ensure complete carbon removal. Phase-pure perovskite PZT was formed on the hot plate at 450 °C after completion of reaction. Figure 1a shows the synthesis steps of making PZT nanoparticles, and Figure 1b shows the complex process of chelation of citric acid with metal ion.

Figure 2 shows the XRD analysis of the PZT powder synthesized using different C/N ratios at different temperatures. The figure shows that phase-pure PZT powder has been formed after calcination at 500 °C for 15 min in the furnace as well as on the hot plate at 450 °C. The XRD data with both 0.5 and 1.5 C/N ratios indicate phase-pure PZT formation at 500 °C. Therefore, C/N ratios in the range of 0.5−1.5 do not have any significant effect on the crystallization temperature of PZT nanoparticles. During heating on the hot plate the exothermic reaction between the citrate and nitrate helps formation of the PZT powder on the hot plate itself. But due to the presence of citric acid some amount of carbon may be present in that powder. Therefore, it is necessary to heat treat the powder at 500 °C for 15 min to remove the carbon completely. Heating for a long time or at a high temperature enhances the chance of agglomeration of nanoparticles.

(35) Fushimi, S.; Ikeda, T. *J. Am. Ceram. Soc.* **1967**, *50* (3), 129–132.

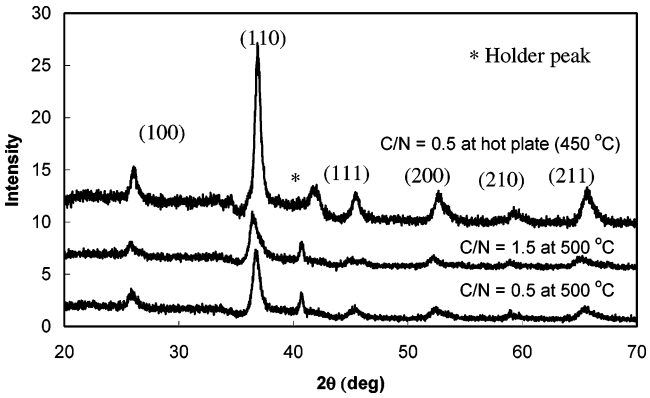


**Figure 2.** XRD plot for the calcined (500 °C/15 min) PZT powder at different citrate-to-nitrate ratios. The plot also shows the uncalcined PZT powder synthesized on a hot plate (450 °C) at a citrate-to-nitrate ratio of 0.5.

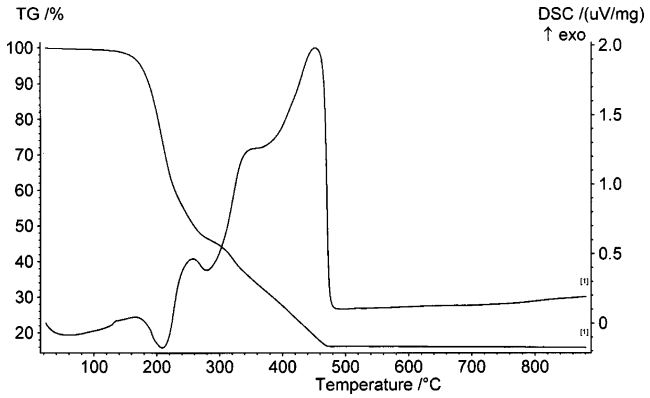


**Figure 3.** DSC/TGA curve for the PZT gel at a citrate-to-nitrate ratio of 0.5.

Figure 3 shows the DSC/TGA plot of the PZT precursor gel made with a citrate-to-nitrate ratio of 0.5. The DSC plot shows that there is a small endothermic peak at a temperature of about 210 °C. This peak is due to the decomposition of excess citrate ions, which decompose endothermically. A further increase in temperature changes the reaction from endothermic to exothermic, which introduces a small exothermic peak at 345 °C and another exothermic peak at 460 °C. The peak at 345 °C may be due to the decomposition of citrate complex and burning of citrate chains. The peak at 460 °C is due to the combustion nature of the reaction between citrate and nitrate groups and burning of residual carbon present in citric acid, which generates a large amount of heat.[31] After this peak there is no peak present in the DSC plot, which indicates that the formation of the PZT phase also takes place within this temperature range. The TGA plot shows there is no weight change after 480 °C, which ensures that no carbon is present above this temperature and all the oxidation and reduction reactions and phase formation take place below this temperature. The XRD data of the phase-pure PZT powder, made on a hot plate, also support the results of the DSC/TGA plot.

Figure 4 shows the effect of the C/N ratio on the BET specific surface area. As the C/N ratio increases the specific surface area increases. But the overall change in surface area is not significant. The lowest surface area is about $2 \pm 0.5$ $m^2/g$ at a C/N ratio of 0.5, and the highest is $4.6 \pm 1$ $m^2/g$ at a C/N ratio of 1.5. This change is very low, which indicates that the C/N ratio does not

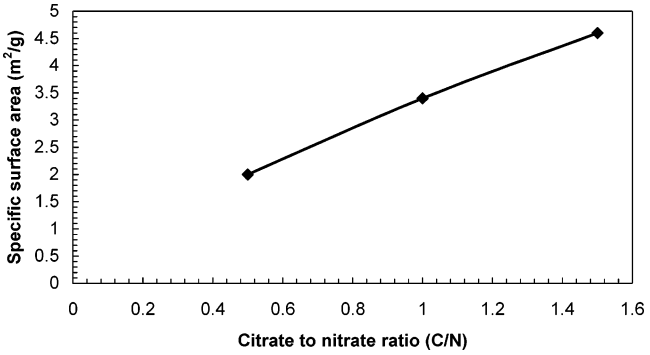


**Figure 4.** BET specific surface area at different citrate-to-nitrate ratios.

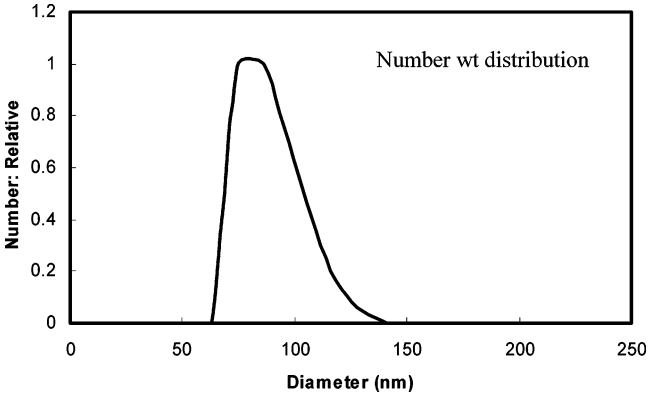


**Figure 6.** Particle size distribution of PZT powder prepared at a citrate-to-nitrate ratio of 0.5.

have a significant effect on the BET specific average surface area of the PZT nanoparticles.

Figure 5 shows the TEM micrographs of these nanoparticles. The morphology changes with increasing C/N ratio as shown in Figure 5. It was found that the different C/N ratios have a significant effect on the morphology of the PZT powder. Figure 5a shows the TEM picture of free-standing PZT nanoparticles at a C/N ratio of 0.5. No clustering or nanoporous-type structure formation can be observed in these particles. The particles are in the size range of 70−110 nm. But increasing the C/N ratio enhances the coagulation of particles and tends to form nanoporous structures. In Figure 5b, where the C/N ratio is 1.0, it can be seen that the particles start to coagulate. Figure 5c shows the agglomerated porous-type structure which is formed at a C/N ratio of 1.5. These TEM pictures also help to explain the increasing trend of the surface area with increasing C/N ratio. By increasing the ratio, the particles form nanoporous structures, which have higher specific surface areas than the free-standing particles. A higher amount of citrate adds more carbon to the system, i.e., supplying more fuel for the reaction, and this high amount of fuel increases the heat generation in the reaction mixture. The presence of excess heat agglomerates the particles.

Figure 6 shows the particle size distribution of the PZT powder prepared at a C/N ratio of 0.5. The plot shows a narrow particle size distribution of the PZT particles in the range of 70−110 nm with an average particle size of 90 nm.

Figure 7 shows the sintering plot of PZT powders prepared with C/N ratios of 0.5 and 1.5. It has been found that the green densities of the pressed pellets of the PZT powder made at a C/N ratio of 0.5 were between 58% and 60% of the theoretical density and those of the pellets made of powder synthesized using a C/N ratio of 1.5 were between 48% and 52% of the theoretical density. The powder synthesized at a C/N ratio of 0.5 gives free-standing nanoparticles of PZT. The free-standing particles have a better packing efficiency and therefore a high green density. The powder synthesized at a C/N ratio of 1.5 gives a porous structured nanopowder of PZT which does not have a high packing efficiency and is responsible for the low green density of about 48−52% of the theoretical density. The plot shows that at the same temperature the powder made at a 0.5 ratio always has a higher density than powder made at a 1.5 ratio, and this is due to the difference in green density. Figure 7 shows that both plots are linear and the slopes are the same up to a temperature of 1150 °C. Then the slope of the curve for the sample where C/N is 0.5 increases sharply compared to that for the sample where C/N is 1.5. This is due to the increased rate of sintering effect. The pure PZT sample shows solid-state sintering at high temperature. The rate of solid-state sintering depends on the particle contact and compactness of the sample. A more compact sample shows a higher sintering rate. At 1200 °C about 97.5% theoretical density is achieved with the powder made at a C/N ratio of 0.5, which is lower than the usual PZT sintering temperature of 1285 °C. The dielectric constant value of the 97.5% sintered sample is about 550 at room temperature, the $d_{33}$ value is 160 pC/N, and the $k_t$ value is 0.35. For ZnO-doped PZT nanoparticles, 0.1, 0.5, 1.0, 1.5, 2.0, and 5 wt % ZnO in PZT were studied. When these PZT nanoparticless were doped with 2 wt % ZnO, the sintering temperature was lowered to 900 °C, with 93% theoretical density. The

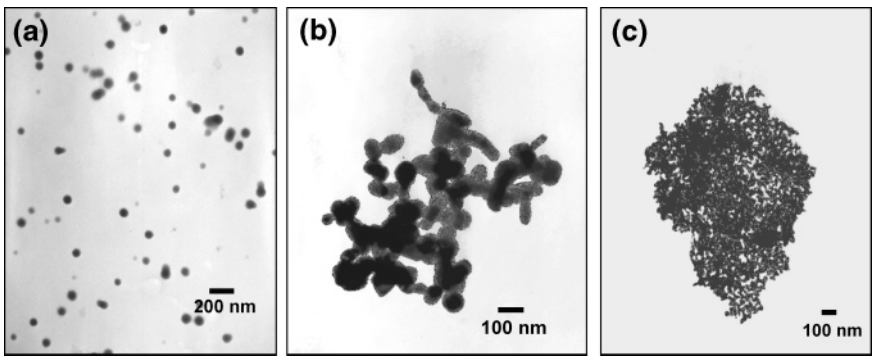


**Figure 5.** TEM picture of PZT powder prepared at a citrate-to-nitrate ratio of 0.5 (a). TEM picture of PZT powder prepared at a citrate-to-nitrate ratio of 1.0 (b). TEM picture of PZT powder prepared at a citrate-to-nitrate ratio of 1.5 (c).

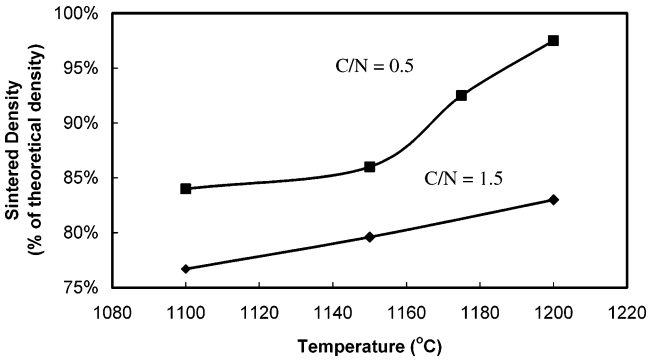


**Figure 7.** Sintering plot for PZT nanoparticles prepared at citrate-to-nitrate ratios of 0.5 and 1.5.

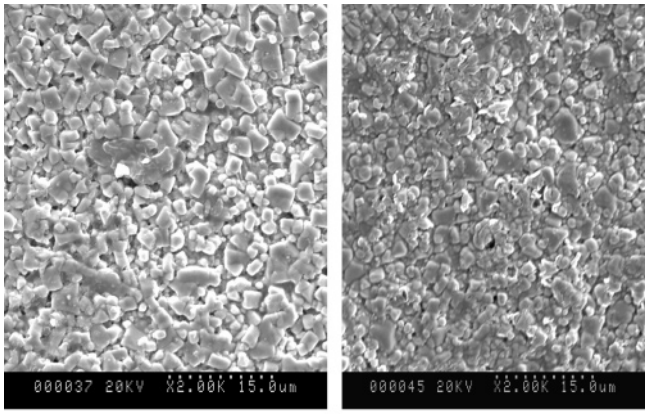


**Figure 8.** Effect of ZnO content on the microstructure of PZT compacts.

presence of a glassy phase along the grain boundary was observed due to ZnO addition, as shown in Figure 8. Formation of low-melting-point eutectics due to the addition of ZnO in PZT may be responsible for the liquid phase during sintering. It was observed that an increase in ZnO content increases the glassy-phase formation. This low-melting-point glassy phase is responsible for low-temperature densification of PZT nanoparticles. The dielectric constants of these nanoparticles were in the range of 1200−1250, which was 2.5 times higher than those of the pure PZT nanoparticles. A piezoelectric constant ($d_{33}$) in the range of 155−170 pC/N and a coupling coefficient ($k_t$) in the range of 0.32−0.34 were measured, which shows that the addition of ZnO did not have any detrimental effect on the piezoelectric properties of PZT.

## Conclusions

Free-standing nanoparticles of PZT have been synthesized successfully by using the citrate nitrate autocombustion method with a narrow particle size distribution in the range of 70−110 nm. Using this autocombustion method, it is possible to synthesize the phase-pure perovskite PZT nanoparticles at a temperature below 500 °C. The ratios of C/N have a significant effect on the morphology of the powder. It has been found that by increasing the C/N ratio the morphology of the PZT nanoparticles changed from free-standing to an agglomerate form. Though the surface area increases with increasing ratio of C/N, it does not have a significant effect. A sintering study of the PZT powder synthesized using the a C/N ratio of 0.5 showed 97.5% densification at 1200 °C for 20 min, compared to the conventional PZT sintering temperature of 1285 °C. The room temperature dielectric constant is 550, the $d_{33}$ value is 160 pC/N, and the $k_t$ value is 0.35. This nanocrystalline PZT powder can be useful for low-temperature sintering on a wide range of substrates. Addition of ZnO along with PZT reduced the sintering temperature to 900 °C compared to 1200 °C of pure PZT nanoparticles. 93% theoretical density was obtained after sintering at 900 °C for 1 h. The room temperature dielectric constants of these nanoparticles were in the range of 1200−1250, the piezoelectric constants in the range of 155−170 pC/N, and coupling coefficients in the range of 0.32−0.34.

**Acknowledgment.** We acknowledge the experimental help with the electromechanical characterization and helpful discussion with Prof. Amit Bandyopadhyay. The work was supported by the National Science Foundation through the Presidential Early Career Award for Scientists and Engineers (PECASE) to S. Bose (under Grant No. CTS-0134476).

CM0490423